

Surface Electronic Structures and Magnetism of a Full-Heusler Alloy $\text{Co}_2\text{CrGa}(001)$: A First-principles Study

Ying Jiu Jin and Jae Il Lee*

Department of Physics, Inha University, Incheon 402-751, Korea

(Received 24 August 2007)

We have investigated the electronic structures and magnetism of a full Heusler alloy $\text{Co}_2\text{CrGa}(001)$ surface by using the all-electron full-potential linearized augmented plane wave (FLAPW) method within the generalized gradient approximation (GGA). We considered two types of different terminations: the Co-terminated (Co-Term) and the CrGa-terminated (CrGa-Term) surfaces. From the calculated layer-projected density of states (LDOS), we found that the surface of the CrGa-Term shows nearly half-metallic character while that of the Co-Term is far from the half-metallic. For the Co-Term, the surface Co atom moves down to the bulk region by 0.05 \AA , while the subsurface Cr and Ga atoms move up to the surface layer by 0.05 and 0.01 \AA , respectively. For the CrGa-Term, there is a large inward relaxation of the surface Ga atom (0.07 \AA), but the relaxation of the surface Cr atom is very small (0.01 \AA). The relaxations affect not much to the overall shapes of DOS for both terminations, but make the surface states of the surface Cr and Ga atoms for the CrGa-Term shift to higher energy that enhances the nearly half-metallic character of the CrGa-Term. The magnetic moments of the surface Cr ($2.98 \mu_B$) in the CrGa-Term and the surface Co ($1.17 \mu_B$) in the Co-Term were much increased compared to those of the inner-layers (1.79 and $0.77 \mu_B$), respectively, while that of the subsurface Cr atom in the Co-Term was decreased to $1.19 \mu_B$.

Keywords : half-metallicity, electronic structure, magnetism, Co_2CrGa

1. Introduction

Half-metallic ferromagnets have attracted much attention because of their potential applications for spintronic devices. The materials have complete (100%) spin-polarization at the Fermi level since one of the spin channel has metallic character while the other shows semiconducting character with a band gap at the Fermi level. Half Heusler alloy NiMnSb is the first material predicted to be half-metallic ferromagnet by de Groot *et al.* in 1983 [1]. Recently, another family of Heusler alloys, the full Heusler alloys have been investigated extensively because many of them were theoretically proposed to be half-metallic ferromagnets with high Curie temperatures and large magnetic moments [2-8]. Actually some of them were experimentally synthesized [9-12]. Full Heusler alloys have chemical formula of X_2YZ , where X and Y are transition metal elements and Z is a group III or IV element in the periodic table. They have $L2_1$ structure

consisted of two interpenetrating zinc-blende XY and XZ compounds, i.e., one of the zinc-blende lattices interpenetrated into the other zinc-blende one with a shift of $1/2(a, a, a)$ where a is a lattice constant of the full Heusler alloy X_2YZ .

Among the full Heusler alloys, Co_2CrGa is regarded to be a promising candidate for spintronic application since it was expected to have almost half-metallic character by band structure calculations [8, 13, 14] and confirmed by an experiment [13]. Band structure calculations using the linear muffin-tin orbital (LMTO) method within the local spin density approximation (LSDA) showed a half-metal-type density of states (DOS) for this compound [8, 13, 14] and the spin-polarization was estimated to be about 95% [13]. According to the classification of the half-metallic materials by Coey *et al.* [15, 16], the Co_2CrGa compound can be classified into the type-III half-metals [8] in which the DOS at the Fermi level is not zero for either spin channel and the majority spin states at the Fermi level are localized, while the minority spin ones delocalized. In experiments, the $L2_1$ -type single phase of Co_2CrGa alloy can be easily synthesized by melting method [13, 17, 18].

*Corresponding author: Tel: +82-32-860-7654,
Fax: +82-32-872-7652, e-mail: jilee@inha.ac.kr

A Curie temperature of 495 K and a saturation magnetic moment of $3.01 \mu_B/\text{f.u.}$ were measured by Umetsu *et al.* [13] using a superconducting quantum interference device (SQUID) magnetometer and a vibrating sample magnetometer (VSM). The saturation magnetic moment follows well the generalized Slater-Pauling rule [4] and it is in consistent with the band structure calculations [8, 13, 14].

The discrepancies between the theoretical predictions and the experimental measurements have been found in many of the half-metallic ferromagnets. The spin-polarization for half Heusler NiMnSb film was measured to be only 58% by the superconducting point contact measurement [19]. Similarly, Singh *et al.* [20] also found that the spin-polarized transport current of the Co_2MnSi thin film was 54% by the point contact Andreev reflection spectroscopy. The discrepancies are attributed to the atomic disorders or the surface effects [21, 22].

For practical applications in spintronics, it is important to have comprehensive understanding on the surface electronic structures of the half-metallic ferromagnets. First-principles calculations for some of the (001) surface of full Heusler alloys were carried out by several researchers. Galanakis [23] investigated the electronic structures and half-metallicity at the (001) surfaces of Co_2MnGe and Co_2CrAl , and he found that all the (001) surfaces are not half-metallic. Hashemifar *et al.* [24] performed *ab initio* calculation for 15 different terminations of $\text{Co}_2\text{MnSi}(001)$ surface and they found that the half-metallicity was destroyed at all the terminations due to the surface states except for the pure Mn termination in which the half-metallicity was preserved by the strong surface-subsurface coupling.

In this study, we investigated the electronic structures and magnetism of the full-Heusler alloy $\text{Co}_2\text{CrGa}(001)$ surface by using the all-electron full-potential linearized augmented plane wave (FLAPW) method within the generalized gradient approximation (GGA). In Sec. II, we describe the calculational model and method. We present the results and discussions in Sec. III, and a brief summary in Sec. IV.

2. Model and Calculational Method

Along the [001] direction of the full Heusler alloy with $L2_1$ structure, there are two types of surface terminations. Hence we considered both terminations, the Co atom terminated (Co-Term) and CrGa atoms terminated (CrGa-Term) surfaces. In order to investigate the surface properties, single slabs with eleven- and thirteen-atomic layers were considered for the Co-Term and the CrGa-Term, respectively. The two-dimensional (2D) lattice con-

stant was taken to be 7.76 a.u. and the interlayer spacings were taken to be 2.74 a.u. which is a quarter of the experimental lattice constant [9]. Surface relaxations were performed from the total energy and atomic force calculations [25]. The equilibrium structures were assumed when the atomic force on each atom becomes less than 2 mRy/a.u.

The Kohn-Sham equation [26] was solved self-consistently in terms of the FLAPW method [27] within the GGA [28] to the exchange-correlation potential. Lattice harmonics with $l \leq 8$ were employed to expand the charge density, potential, and wavefunctions inside the muffin-tin (MT) radius of 2.35 a.u. for the Cr atom and 2.10 a.u. for the Co and Ga atoms, respectively. A plane wave cutoff of 14 Ry was employed for the LAPW basis, corresponding to about 2000 and 2400 LAPW functions for the Co-Term and the CrGa-Term, respectively. A 200 Ry star-function cutoff was used to depict the charge density and potential in the interstitial region. Integrations inside the Brillouin zone (BZ) were performed by a summation over a 12×12 mesh which correspond to 21 \mathbf{k} -points inside the $1/8$ wedge of the irreducible 2D BZ. All core electrons were treated fully relativistically, while valence states were treated scalar relativistically, i.e., not taking account of the spin-orbit coupling [29]. Self-consistency was assumed when the difference between the input and the output charge (spin) density was less than 1.0×10^{-4} electrons/a.u.³

3. Results and Discussion

The calculated amount of relaxations with respect to the bulk position is given in Table 1 for the Co-Term and CrGa-Term in units of Å. The sign of + and – denote the outward and the inward relaxations, respectively. We used S, S-I, and C to denote the surface, subsurface, and center layers.

It is found that the surface atoms for both terminations relaxed inward similarly to many cases of transition metals [30-32], while the subsurface atoms move outward, regardless of the termination. The inward relaxations of the surface atoms can be qualitatively understood by the charge-smoothing model proposed by Finnis and Heine [33]. When a surface is created, electrons in the surface atoms move to vacuum and hollow sites in order to reduce electron kinetic energy which causes inward electrostatic forces on the surface atoms to move inward.

We found that the CrGa-planes in both terminations tend to form buckling geometry. At the surface of the CrGa-Term, the inward relaxation of surface Cr atom (0.01 Å) is smaller than that of the surface Ga atom (0.07

Table 1. The calculated amount of relaxations with respect to the bulk position for the Co-Term and CrGa-Term in units of Å. The sign of + and - denote the outward and inward relaxations, respectively.

Co-term		CrGa-term	
atom (layer)	Δd	atom (layer)	Δd
		Cr(S)	-0.01
		Ga(S)	-0.07
Co(S)	-0.05	Co(S-1)	+0.03
Cr(S-1)	+0.05	Cr(S-2)	-0.03
Ga(S-1)	+0.01	Ga(S-2)	-0.02
Co(S-2)	-0.03	Co(S-3)	-0.04
Cr(S-3)	+0.01	Cr(S-4)	-0.01
Ga(S-3)	0.00	Ga(S-4)	-0.01
Co(S-4)	+0.03	Co(S-5)	+0.03
Cr(C)	0	Cr(C)	0
Ga(C)	0	Ga(C)	0

Å), making a buckling of 0.06 Å. The smaller relaxation of surface Cr atom was considered due to the magnetic dipole-dipole repulsion between the surface Cr and subsurface Co atoms. The amount of buckling of the deep inner CrGa-planes were very small for both terminations. The amount (0.05 Å) of the inward relaxation for the surface Co atom of the Co-Term is close to that (0.06 Å) of the Co(0001) surface obtained by band structure calculation [34]. For both termination, the absolute values of displacements of the Co atoms in the inner layers are nearly same as 0.3 Å.

The spin-polarized layer-projected density of states (LDOS) for (a) the Co-Term and (b) the CrGa-Term were presented in Figure 1. The LDOS values for Ga atoms were multiplied by 10 for convenience and the LDOS values of the spin down states were multiplied by -1. The Fermi levels were set to zero. The solid and dotted lines denote the relaxed and the unrelaxed systems, respectively. We found that in the deep inner layers the surface relaxations for both terminations did not change significantly the overall shapes of the LDOSs. At the center-layers in both systems, the Fermi levels locating at the edge of the minority spin gap displays that the center layers of both terminations are almost half-metallic consistently with the previous band structure calculations for bulk Co_2CrGa [8, 13, 14].

At the surface layer of Co-Term, as can be seen in Figure 1(a), the majority and minority spin Co(S) *d*-states become narrower compared to those of the deep inner layer of Co(S-4). The occupied minority spin Co(S) *d*-states were shifted to higher energy region due to the reduced coordination number and symmetry breaking at the surface. We have calculated the surface spin-polarization

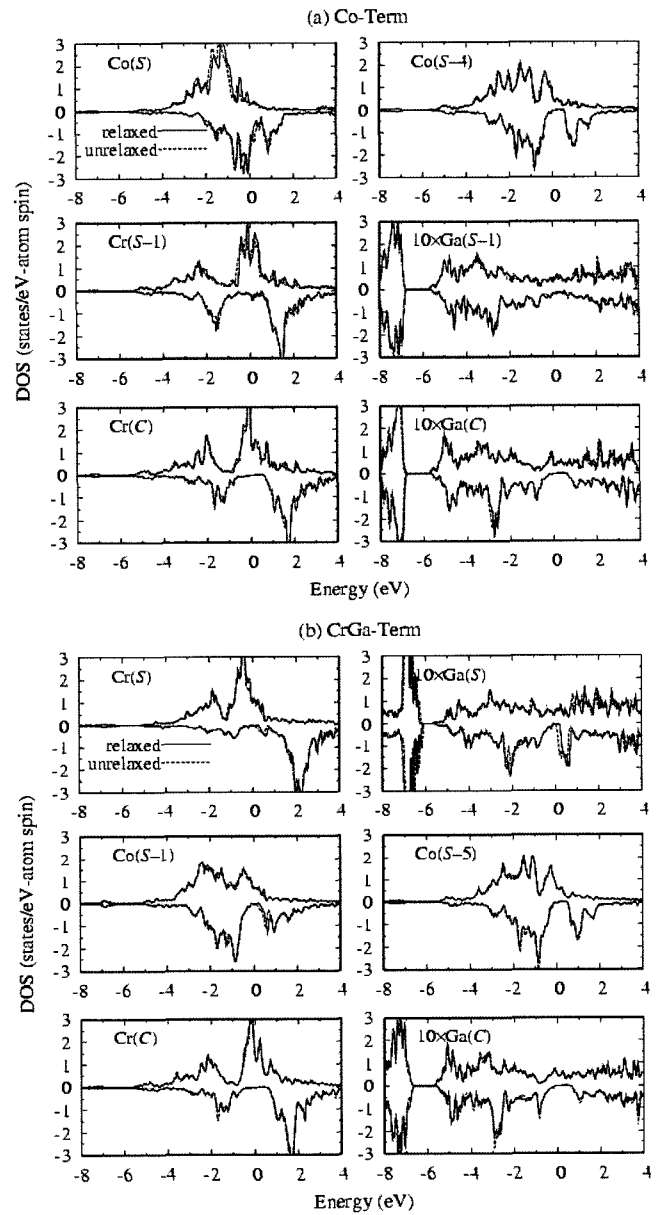


Fig. 1. The spin polarized layer-projected density of states for (a) the Co-Term and (b) the CrGa-Term. The values of the LDOS of Ga atoms are multiplied by 10 and the LDOS values of the spin down states are multiplied by -1. The Fermi levels are set to zero. The solid and dotted lines denote relaxed and unrelaxed systems, respectively.

of the P1 and P2 from the ratio of the difference between the majority and minority spin DOS versus the total DOS at the Fermi level. The P1 and P2 are calculated by taking into account the LDOS of the surface layer only and both the surface and subsurface layers, respectively. Since the Fermi level locates just below the large peak of the minority spin Co(S) 3d-LDOS, the surface spin-polarization ($P1 = -63\%$) is negative so that it is opposite to that of the center layer. Similar behavior

was also found for the Co terminated surfaces of $\text{Co}_2\text{CrAl}(001)$ [23] and $\text{Co}_2\text{MnSi}(001)$ [35]. After relaxation, the minority spin states of Co(S) near the Fermi level shift a little to lower energy to reduce the minority spin DOS at the Fermi level, while the majority spin states of Co(S) around 1.5 eV below the Fermi level move a little towards higher energy. In the subsurface layer, the Cr and Ga atoms have considerably large minority spin LDOS at the Fermi level due to the hybridizations with the minority spin d-states of the surface Co atom. It is also found that the spin splitting of d-bands of the Cr(S-1) is reduced slightly compared with that of the center layer Cr(C) due to the enhanced hybridizations with the surface Co atom, and it makes a reduction in the magnetic moment of Cr(S-1).

For the CrGa-Term (see Fig. 1(b)), we found that a localized surface states located at ~ 0.2 eV above the Fermi level for the minority spin states of the Cr(S) and Ga(S) atoms, which destroys the minority spin band gap in bulk state. The minority spin LDOSs of the Cr(S) and Ga(S) at the Fermi level were almost vanished which results in high surface spin-polarizations of 92 and 89% for the P1 and P2, respectively. This behavior is similar to the case of the CrAl-terminated surface of $\text{Co}_2\text{CrAl}(001)$ [23] in which the surface spin-polarization of P2 is 84 %, but it is different to the case of the MnSi-terminated surface of $\text{Co}_2\text{MnSi}(001)$ in which minority surface states appeared at the Fermi level [24]. The surface spin-polarization of P2 is -16% . For the Cr(S), both the majority and minority spin states become narrowed and the spin splitting of the d-bands was increased with respect to that of the Cr(C) by the surface effect. For the subsurface Co(S-1), a new minority spin peak appeared around 0.6 eV above Fermi level due to the hybridization with the surface atoms, but the general shape of the minority spin LDOS below the Fermi level was not changed much compared with that of the inner layer Co(S-5). When the system was relaxed, the hybridizations between the surface and subsurface atoms were enhanced due to the decreased bond lengths, and consequently the surface states of the Cr(S) and Ga(S) atoms move to higher energy regions that enhances the nearly half-metallic character at the surface of the CrGa-Term.

In order to understand the electronic and magnetic properties in detail, we presented the layer projected l -decomposed majority and minority spin electrons inside each MT sphere and the calculated magnetic moments for the relaxed systems in Table 2 as well as the spin density contour plots: (a) the (200) plane of the Co-Term and (b) the (220) plane of the CrGa-Term for the relaxed systems in Fig. 2. The solid and the broken lines represent

Table 2. The layer-projected l -decomposed majority and minority spin-electrons inside each muffin-tin spheres, layer-by-layer magnetic moments (in units of μ_B), and the surface spin polarization of P.

the CrGa-Term					
atom(layer)	$s(\uparrow/\downarrow)$	$p(\uparrow/\downarrow)$	$d(\uparrow/\downarrow)$	total(\uparrow/\downarrow)	M
Cr(S)	0.15/0.12	0.11/0.10	3.50/0.56	3.77/0.79	2.98
Ga(S)	0.35/0.35	0.24/0.27	4.91/4.91	5.51/5.54	-0.03
Co(S-1)	0.14/0.14	0.12/0.14	3.91/3.13	4.18/3.40	0.78
Cr(S-2)	0.16/0.15	0.16/0.17	2.92/1.10	3.27/1.44	1.83
Ga(S-2)	0.32/0.32	0.28/0.31	4.92/4.92	5.52/5.56	-0.04
Co(S-3)	0.14/0.14	0.13/0.14	3.88/3.14	4.16/3.43	0.73
Cr(S-4)	0.17/0.16	0.17/0.18	2.79/1.24	3.15/1.60	1.55
Ga(S-4)	0.32/0.32	0.29/0.32	4.92/4.92	5.54/5.58	-0.04
Co(S-5)	0.14/0.14	0.12/0.14	3.89/3.13	4.17/3.41	0.75
Cr(C)	0.15/0.16	0.17/0.17	2.90/1.12	3.24/1.46	1.79
Ga(C)	0.32/0.32	0.28/0.31	4.92/4.92	5.52/5.57	-0.04
P1			$\sim 92\%$		
P2			$\sim 89\%$		
the Co-Term					
Co(S)	0.14/0.13	0.08/0.08	4.09/2.93	4.31/3.14	1.17
Cr(S-1)	0.16/0.16	0.17/0.17	2.60/1.40	2.95/1.76	1.19
Ga(S-1)	0.31/0.32	0.28/0.32	4.92/4.92	5.53/5.57	-0.05
Co(S-2)	0.14/0.14	0.12/0.14	3.91/3.11	4.18/3.39	0.79
Cr(S-3)	0.16/0.16	0.17/0.18	2.76/1.26	3.12/1.62	1.50
Ga(S-3)	0.32/0.32	0.29/0.32	4.92/4.92	5.53/5.58	-0.04
Co(S-4)	0.14/0.14	0.12/0.14	3.90/3.12	4.17/3.40	0.77
Cr(C)	0.16/0.15	0.17/0.17	2.90/1.12	3.25/1.46	1.79
Ga(C)	0.32/0.32	0.28/0.31	4.92/4.92	5.52/5.57	-0.04
P1			$\sim -63\%$		
P2			$\sim 0\%$		

positively and negatively polarized spin densities, respectively. The lowest contour starts from 1×10^{-3} electrons/a.u.³ and the subsequent lines differ by a factor of $\sqrt{2}$. From the Table 2, we found that the Co(S) atom for the Co-Term loses 0.1 p-like electrons and the Cr(S) and Ga(S) atoms for the CrGa-Term lose 0.13 and 0.08 p-like electrons, respectively. Those p-like electrons spill out into the vacuum region to screen the surface termination as seen in Fig. 2. In both terminations, the numbers of d-electrons of the Co and Cr atoms are nearly constants of 7.02 and 4.02, respectively.

The magnetic moments of the Cr(S) in the CrGa-Term and the Co(S) in the Co-Term were calculated to 2.98 and 1.17 μ_B , respectively, which were 66 and 52% larger than that of the deep inner layers due to the band narrowing and the enhanced spin-splitting at the surfaces. The results are consistent with the large eruptions of majority spin contours from the Co(S) in the Co-Term and Cr(S) in the CrGa-Term as shown in Fig. 2. On the other hand, the magnetic moment of Cr(S-1) atom in the Co-Term was

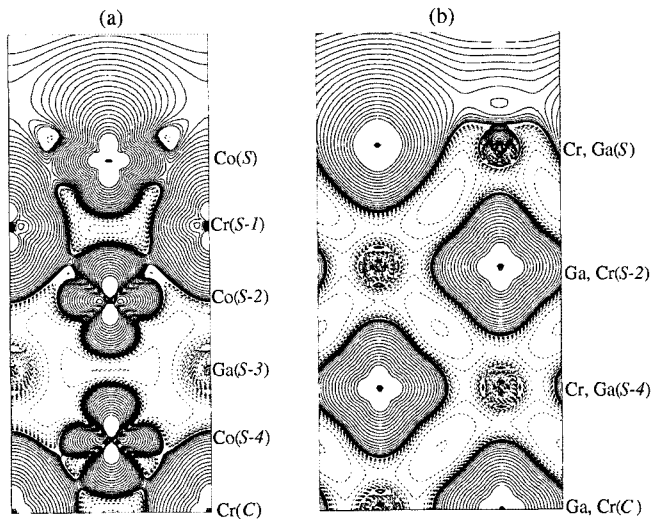


Fig. 2. The spin density contour plots for the relaxed systems in (a) the (200) plane of the Co-Term and (b) the (220) plane of the CrGa-Term. The solid and the broken lines represent positively and negatively polarized spin densities, respectively. The lowest contour starts from $\pm 1 \times 10^{-3}$ electrons/a.u.³ and the subsequent lines differ by a factor of $\sqrt{2}$.

decreased to $1.19 \mu_B$ due to the increased d-d hybridization between the Cr(S-1) and Co(S) atoms. The magnetic moments of Co atoms in the deep inner layers for both terminations are calculated to $\sim 0.75 \mu_B$ which is close to those of the bulk ($0.75 \mu_B$) [8] and the experimental value ($0.80 \mu_B$) [14]. The magnetic moment, $1.79 \mu_B$, of Cr atoms in the center layers of both terminations are slightly larger than the bulk value $1.63 \mu_B$ [8], but considerably larger than that of the experiment, $1.1 \mu_B$ [14]. The magnetic moments of Ga atoms, which are almost zero, are antiferromagnetically coupled with the Co atoms.

4. Summary

We investigated the electronic structures, half-metallicity and magnetism of the $\text{Co}_2\text{CrGa}(001)$ surface by using the all-electron FLAPW method within the GGA to the exchange-correlation potential. Two possible terminations of Co-Term and CrGa-Term were considered. From the calculated LDOS, we found that the CrGa-Term is nearly half-metallic while the Co-Term is far from the half-metallic. We determined the relaxed structures by total energy and atomic force calculations for both of the Co-Term and CrGa-Term surfaces. For the Co-Term, the surface Co atom moves down to the bulk region by 0.05 \AA , while the subsurface Cr and Ga atoms move up to the surface layer by 0.05 and 0.01 \AA , respectively. For the CrGa-term, there is an inward relaxation of the surface

Ga atom (0.07 \AA), but the relaxation of the surface Cr atom is very small (0.01 \AA) which makes a buckling of 0.06 \AA . The relaxations do not affect significantly to the overall shapes of DOS for both terminations. After relaxation, the surface states of the surface Cr and Ga atoms of the CrGa-Term shift a little to higher energy which enhances the half-metallic character. At the surface, the magnetic moment of Cr ($2.98 \mu_B$) for the CrGa-Term and Co ($1.17 \mu_B$) for the Co-Term are much enhanced compared with those of the inner-layers (1.79 and $0.77 \mu_B$), respectively. On the other hand, the magnetic moment of Cr(S-1) atom in the Co-Term was decreased to $1.19 \mu_B$.

References

- [1] R. A. de Groot, F. M. Mueller, P. G. van Engen, and K. H. J. Buschow, *Phys. Rev. Lett.* **50**, 2024 (1983).
- [2] J. Kübler, A. R. Williams, and C. B. Sommers, *Phys. Rev. B* **28**, 11745 (1983).
- [3] S. Picozzi, A. Continenza, and A. J. Freeman, *Phys. Rev. B* **66**, 094421 (2002).
- [4] I. Galanakis, P. Mavropoulos, and P. H. Dederichs, *J. Phys. D: Appl. Phys.* **39**, 765 (2006).
- [5] S. C. Lee, T. D. Lee, P. Blaha, and K. Schwarz, *J. Appl. Phys.* **97**, 10C307 (2005).
- [6] X. Q. Chen, R. Podloucky, and P. Rogl, *J. Appl. Phys.* **100**, 113901 (2006).
- [7] Y. J. Jin and J. I. Lee, *J. Korean Phys. Soc.* **51**, 155 (2007).
- [8] H. C. Kandpal, G. H. Fecher, and C. Felser, *J. Phys. D: Appl. Phys.* **40**, 1507 (2007).
- [9] K. H. J. Buschow, P. G. van Engen, and R. Jongebreur, *J. Magn. Magn. Mater.* **38**, 1 (1983).
- [10] R. J. Kim, Y. J. Yoo, K. K. Yu, T.-U. Nahm, Y. P. Lee, Y. V. Kudryavtsev, V. A. Oksenenko, J. Y. Rhee, and K. W. Kim, *J. Korean Phys. Soc.* **49**, 996 (2006).
- [11] S. Wurmehl, G. H. Fecher, H. C. Kandpal, V. Ksenofontov, C. Felser, H. J. Lin, and J. Morais, *Phys. Rev. B* **72**, 184434 (2005).
- [12] U. Geiersbach, A. Bergmann, and K. Westerholt, *J. Magn. Magn. Mater.* **240**, 546 (2002).
- [13] R. Y. Umetsu, K. Kobayashi, R. Kainuma, A. Fujita, K. Fukamichi, K. Ishida, and A. Sakuma, *Appl. Phys. Lett.* **85**, 2011 (2004).
- [14] S. Ishida, S. Sugimura, S. Fujii, and S. Asano, *J. Phys.: Condens. Matter* **3**, 5793 (1991), and references therein.
- [15] J. M. D. Coey, M. Venkatesan, and M. A. Bari, *Lecture Notes in Physics* **595**, 377 (2002).
- [16] C. Felser, G. H. Fecher, and B. Balke, *Angew. Chem.* **46**, 668 (2007).
- [17] R. Y. Umetsu, K. Kobayashi, A. Fujita, K. Oikawa, R. Kainuma, K. Ishida, N. Endo, K. Fukamichi, and A.

- Sakuma, *Phys. Rev. B* **72**, 214412 (2005).
- [18] K. Kobayashi, R. Y. Umetsu, A. Fujita, K. Oikawa, R. Kainuma, K. Fukamichi, and K. Ishida, *J. Alloy. Compd.* **399**, 60 (2005).
- [19] R. J. Soulen Jr., J. M. Byers, M. S. Osofsky, B. Nadgorny, T. Ambrose, S. F. Cheng, P. R. Broussard, C. T. Tanaka, J. Nowak, J. S. Moodera, A. Barry, and J. M. D. Coey, *Science* **282**, 85 (1998).
- [20] L. J. Singh, Z. H. Barder, Y. Miyoshi, Y. Bugoslavsky, W. R. Branford, and L. F. Cohen, *Appl. Phys. Lett.* **84**, 2367 (2004).
- [21] M. C. Kautzky, F. B. Mancoff, J. F. Bobo, P. R. Johnson, R. L. White, and B. M. Clemens, *J. Appl. Phys.* **81**, 4026 (1997).
- [22] D. Ristoiu, J. P. Nozières, C. N. Borca, B. Borca, and P. A. Dowben, *Appl. Phys. Lett.* **76**, 2349 (2000).
- [23] I. Galanakis, *J. Phys.: Condens. Matter* **14**, 6329 (2002).
- [24] S. J. Hashemifar, P. Kratzer, and M. Scheffler, *Phys. Rev. Lett.* **94**, 096402 (2005).
- [25] W. Mannstadt and A. J. Freeman, *Phys. Rev. B* **55**, 13298 (1997).
- [26] W. Kohn and L. J. Sham, *Phys. Rev.* **140**, A1133 (1965).
- [27] E. Wimmer, H. Krakauer, M. Weinert, and A. J. Freeman, *Phys. Rev. B* **24**, 864 (1981), and references therein; M. Weinert, E. Wimmer, and A. J. Freeman, *ibid.* **26**, 4571 (1982).
- [28] J. P. Perdew, K. Burke, and M. Ernzerhof, *Phys. Rev. Lett.* **77**, 3865 (1996); *ibid.* **78**, 1396(E) (1997).
- [29] D. D. Koelling and B. N. Harmon, *J. Phys. C* **10**, 3107 (1977).
- [30] R. P. Gupta, *Phys. Rev. B* **23**, 6265 (1981).
- [31] M. Methfessel, D. Hennig, and M. Scheffler, *Phys. Rev. B* **46**, 4816 (1992).
- [32] P. J. Feibelman, *Surf. Sci.* **360**, 297 (1996).
- [33] M. W. Finnis and V. Heine, *J. Phys. F: Metal Phys.* **4**, L37 (1974).
- [34] L. G. Wang, E. Y. Tsymbal, and S. S. Jaswal, *J. Magn. Mater.* **286**, 119 (2005).
- [35] S. Ishida, T. Masaki, S. Fujii, and S. Asano, *Physica B* **245**, 1 (1998).